UKAEA FUS 411

EURATOM/UKAEA Fusion

Torque Balance and Rotational Stabilisation of the Resistive Wall Mode

G Gimblett and R J Hastie

May 1999

EURATOM/UKAEA Fusion Association

Culham Science Centre, Abingdon
Oxfordshire, OX14 3DB
United Kingdom
Telephone +44 1235 463311
Facsimile +44 1235 463647

Torque Balance and Rotational Stabilisation of the Resistive Wall Mode

C. G. Gimblett and R. J. Hastie

EURATOM/UKAEA Fusion Association, Culham Science Centre
Abingdon, Oxon, OX 14 3DB, United Kingdom

Abstract

We have investigated a non-linear model of the rotational stabilisation of the Resistive Wall Mode (RWM). Central to the model is a cylindrical plasma that is ideal MHD unstable in the absence of a wall, and possesses an internal resonance (J. M. Finn, Phys. Plasmas **2**, 198 (1995)). This system is then a qualitative model for the actual toroidal external kink mode that is relevant in Advanced Tokamak scenarios. It has been shown in the past that the RWM can possess stability windows for modest rotation frequencies. However, the equilibrium parameter regime in which stabilisation can take place is small. We present a non-linear formulation of the problem, with plasma rotation determined self-consistently by an equation of torque balance. It is found that, within the same small parameter regime, stability windows can be considerably extended at the expense of the growth of a magnetic island. On the other hand, depending on the initial rotation, the system can reduce the plasma rotation rate asymptotically to zero while the island continues to grow.

PACS: 52.30.-q, 52.35.Py, 52.55.Fa

I. Introduction

It is generally accepted that Advanced Tokamak (AT) equilibria require wall stabilisation in order to benefit from the optimised central shear and produce attractive β limits.[1,2] In other words, they must achieve the β limits that are predicted when the surrounding wall is perfectly conducting.[3] However, if the actual finite resistivity of the wall is taken into account, the Resistive Wall Mode (RWM) can be destabilised.[4] Advanced Tokamaks will be particularly vulnerable to this mode, as the flat current density profile in the core indicates that the external kink version of the RWM can be present.

Much work on the RWM in the past has been in the context of the Reversed Field Pinch (RFP). This was at the stage of RFP research when pulse lengths were becoming comparable to wall (vertical field) penetration times. In HBTX1C[5] it was reported that wall locked perturbations were observed to grow (on the wall time) to large amplitude ($\delta b/B_0 \sim 10\%$) and lead to discharge termination due to the large non-Spitzer loop voltage caused by field penetration of the wall. The observed mode numbers, growth rate, and wall locking of these perturbations all appeared to agree with linear theoretical predictions of the RWM, making a good case for their positive identification in this experiment. Observation of the RWM was also reported in Ref. 6. In contrast, Ref. 7 reported experiments on the OHTE 'thin shell' RFP which displayed pulse lengths greatly exceeding the wall time. This was later interpreted as being due to the formation, in OHTE, of a so-called 'slinky' mode (a phase coherence phenomenon) that allowed the RWM to be somehow rearranged and removed. This intriguing situation has not been resolved, due in part to the discontinuation of the two experiments involved.

Early in the theoretical analysis of the RWM it was realised that bulk plasma rotation might have an important effect. If the plasma was modelled as a rotating current-carrying helical wire, for instance, then we would expect suppression of the magnetic flux entering the wall by the classical skin effect. On the other hand, a real plasma has more degrees of freedom than a wire and can 'choose' to lock its perturbation to the wall and vitiate such skin effect. In Ref. 4 it was shown that an ideal RWM in cylindrical geometry did indeed lock to the wall for sub-Alfvénic plasma rotation. Further, when the rotation approached Alfvénic, the effect of inertia was initially to increase the RWM growth rate (in fact a

stable RWM could be destabilised by this effect - see Ref. 8 for a recent investigation). When the rotation was trans-Alfvénic the growth rate did decrease, but there was always a residual instability. In contrast, for a RWM that was resistive in origin, and thereby created a magnetic island at an internal plasma resonance (*e.g.* a tearing mode[9]), the interaction between the island and the wall now permitted stabilisation of the mode, typically when

$$\Omega \sim \mathcal{O}(1/\tau_W) + \mathcal{O}(1/\tau_L) , \tag{1}$$

where Ω is the plasma rotation frequency, τ_L is the tearing layer characteristic time,[9] and τ_W is the wall time. These rotation frequencies are, of course, generally much less than the Alfvén frequency.

In the case of AT equilibria, the important RWM is the one that derives from the pressure driven toroidal ideal external kink mode. Moreover, although the mode is 'ideal' in nature, unlike a cylindrical kink the toroidicity of the mode means that in general there will be a sideband component of the instability that will possess a resonance in the plasma. There is, then, the immediate possibility that a stabilisation mechanism similar to that leading to eqn.(1) exists in the AT.

This possibility was first investigated in a series of papers due to Finn.[10] At the centre of his analysis was the construction of a model *cylindrical* equilibrium that was ideally MHD unstable yet possessed a resonance at some radius. It should be noted that this is not a common occurrence in cylindrical plasmas and requires atypical equilibrium profiles. Nevertheless, the model is useful in producing qualitative results for the full toroidal case. In this report we show how to produce a standard representation of the Finn model, and use it as a basis for the subsequent analysis. The Finn papers, which do indeed display stability windows (in rotation, wall placement *etc.*) for the RWM, deal with linearised MHD and the plasma rotation is an undetermined parameter of the model. We extend this to the non-linear case by considering the torque balance equation, which is used to self-consistently determine the plasma rotation rate.

The motivation for this theoretical research comes from experimental results obtained on the DIII-D experiment.[11] It is possible to calculate the β limit that the RWM would impose on the plasma by using an ideal MHD stability code that uses the boundary

condition that there is no wall at all. Using the normalised $\beta_N = \beta(\%)a(m)B(T)/I(MA)$ (a, B, I the minor radius, toroidal field and current), the RWM β_N limit is shown as the dotted line in the bottom section of Fig. 1. The middle section shows the magnetic perturbation ($m/n = 3/1$) signal and comparing the two sections we see that the RWM starts to develop when β_N exceeds that limit.

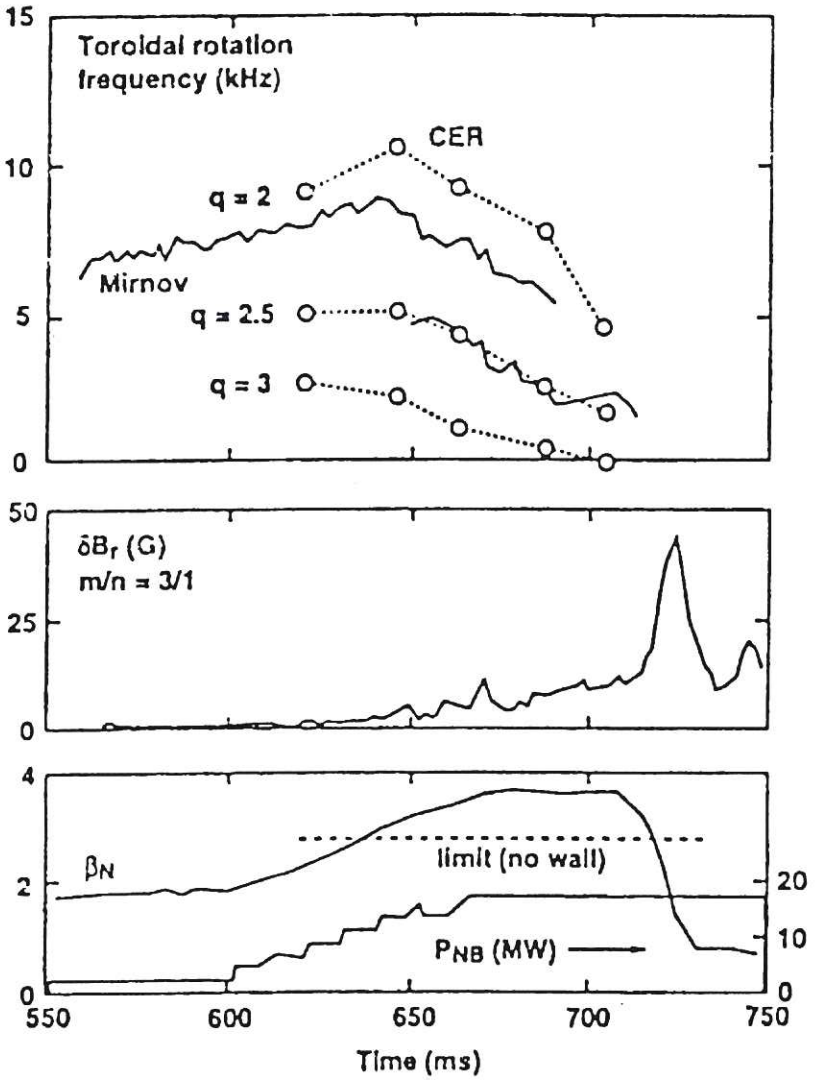

Figure 1: Experimental results from DIII-D

However, the rotation at the $q = 3$ surface (top section of Fig. 1) appears to suppress the mode for a while. Note in passing that the observed rotation rate is a few kHz, and this is orders of magnitude less than the Alfvén frequency ($\sim$ a few MHz). Then we see that even though the Neutral Beam injection power is held constant the rotation starts to decrease, the mode grows in a corresponding manner, and eventually enters a rapidly

growing phase on the wall time scale (~ 5 ms). Thereafter the high β_N phase terminates owing to confinement deterioration.

The suggestion that plasma rotation, if it can be maintained, leads to RWM stabilisation motivated various theoretical models attempting to explain this. A review of these models is to be found in Ref. 12. In summary, many of these models invoke a dissipation mechanism of some sort and it would appear that, with very few exceptions, either the rotation rate or dissipation required for RWM stabilisation is too large to account for the actual DIII-D results. So, the Finn model merits further investigation, in principle providing stability at realistic slow rotation rates. In Sec. II we present a standard form of the model, and Sec. III studies the different types of linear stability window within this generic representation. Then in Sec. IV, we discuss the torque balance equation, a non-linear or quasi-linear effect, that self-consistently determines the fluid rotation rate. These two aspects of the problem, torque balance and stability windows, are then brought together in this section. We discuss the implications of this work for rotational stabilisation of the RWM in AT scenarios in a final Conclusions and Discussion section.

II. A standard form of the Finn model

As remarked above, Ref. 10 modelled a toroidal instability in a cylinder by constructing equilibria that were ideal MHD unstable, and yet a resonance existed in the plasma. This required non-standard current (and hence safety factor, q) profiles. We point out that a somewhat generic formulation of this is possible. The technique is examined in detail in Ref. 12, so it is simply outlined here. The equation that determines the MHD eigenfunction in a cylindrical plasma is a second order ordinary differential equation. It follows that different radial stations in the plasma are 'connected' by this equation in a simple way. The radial stations of interest in our problem are the resonance (where a resistive layer response is formed[9]) and the wall itself, where a simple 'thin shell' response is appropriate.[4] Collating all this information and assuming $\exp(pt)$ time dependence, we can find the standard dispersion relation

$$(p\tau_L)^{5/4} = \frac{1-\delta p\tau_W}{-\epsilon + p\tau_W} . \qquad (2)$$

The left hand side is the plasma response at the resonance, with τ_L the characteristic resistive layer time.[9] This is related to the wall response, $p\tau_W$, as shown on the right hand side. To ensure we have an unstable RWM we require ideal instability if there were no wall ($\tau_W \to 0$), implying $\epsilon > 0$. Indeed, the appropriate response at the layer in this case is the ideal inertial one, $-1/(p\tau_A)$, with τ_A the Alfvén time. So, ϵ is a direct measure of the ideal growth rate in the absence of a wall. If the wall were perfectly conducting ($\tau_W \to \infty$) we see that $-\delta$ gives the stability of the tearing mode in this case (positive δ corresponding to a stable tearing mode). The Finn dispersion relation is indeed of the form given in eqn.(2); in his case ϵ and δ are directly computable from the equilibrium parameters. So, the results we obtain using eqn.(2) will apply to Finn's equilibria.

III. Stability structures within the standard model

The relatively simple dispersion relation, eqn.(2), displays considerable structure which we now investigate. For a non-rotating plasma, eqn.(2) with ϵ and δ both positive always yields an unstable root ($\mathcal{R}(p) > 0$ with $\mathcal{R}$ denoting real part), and this is the RWM. The natural question to ask is how does the mode behave when the plasma is rotating (to simulate this, we can simply Doppler-shift $p \to p - i\Omega$ in the left hand side of eqn.(2), where Ω is the bulk plasma rotation frequency). For the moment we treat Ω as a free parameter, and return to its self-consistent determination in the next section (Sec. IV). As in Ref. 12 we can note that if the RWM were ever to stabilise (the obvious question of interest) then there would have to be a point, as Ω increases, at which p was purely imaginary, $p = i\omega$ with ω real. Inserting this into eqn.(2) it was shown that this implied a necessary condition for the existence of such marginal points was

$$0 < \quad \epsilon\delta \quad < 0.04 \; . \tag{3}$$

This is, essentially, the statement that a necessary condition for stabilising the RWM is that the ideal mode in the absence of a wall (growth rate $\sim \epsilon$) should not be too unstable, while similarly the tearing mode which exists when the wall is perfect (growth rate determined by δ) be only weakly stable. The smallness of this region of $\epsilon - \delta$ space implies stringent conditions on specific equilibria.

In fact, if eqn.(3) is obeyed there are exactly *two* marginal points. This information, by itself, does not guarantee the existence of a stable window in Ω. In fact, extensive numerical investigation of eqn.(2) in the parameter regime of eqn.(3) revealed that four different topologies exist as roots are tracked with increasing Ω. To recap, when $\Omega = 0$ there are three physically acceptable roots of eqn.(2). The RWM is a non-rotating mode associated with the wall; the two other roots are stable 'backward' (b) and 'forward' (f) rotating stable tearing modes associated with the resistive layer. When Ω is increased, the forward mode (rotating in the same sense as the RWM) always remains stable and never achieves marginality.

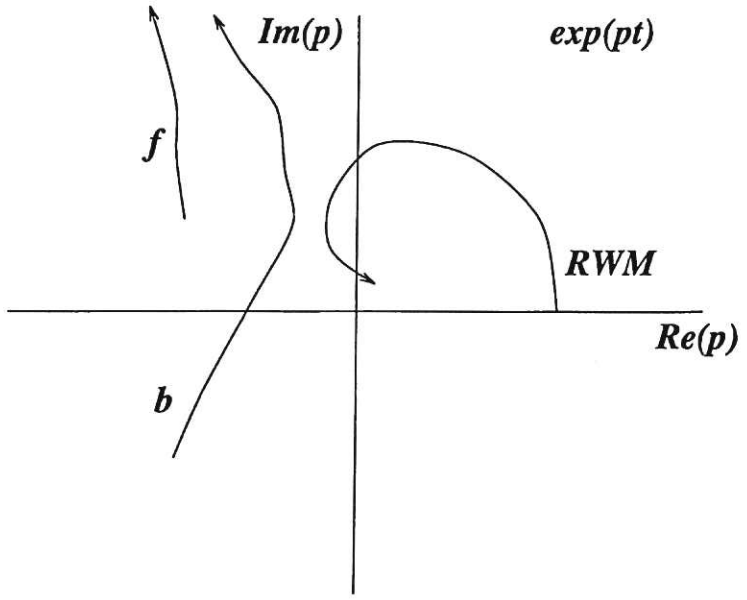

Figure 2: A stability window for the RWM

Figure 2 shows schematically the locus of the three roots as Ω increases for the case $\epsilon = 0.05, \delta = 0.5$. Here we see that the f and b roots remain stable. The RWM is the root that possesses the two marginal points, and a stability window in Ω is encountered. If we now hold ϵ at 0.05 and reduce δ to 0.25, then the topology of the loci of Fig. 2 changes. This topology change occurs *via* a 'reconnection' of the RWM and b modes - and this in turn requires the existence of a double root, see below for a discussion. The two marginal points are now shared between the RWM and b mode and Fig. 3 shows the schematic tracks of the three roots for this case.

Although the topology changes, a stability window *still* exists in this case as the

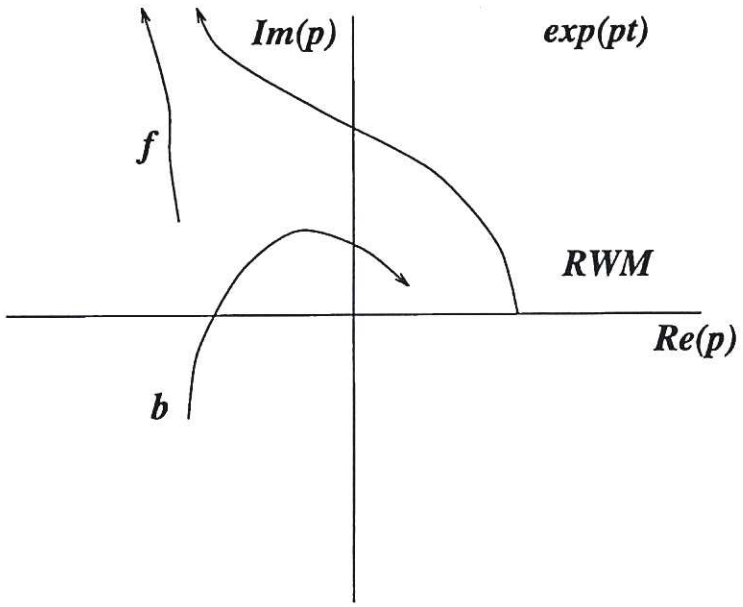

Figure 3: A stability window shared between the RWM and the 'backward' mode

rotation frequency Ω_1 at which the RWM stabilises is less than the rotation frequency Ω_2 at which the b mode destabilises. However, as we continue to reduce δ, this window shrinks until eventually $\Omega_1 = \Omega_2$ and the window disappears (this is discussed further below). Further reduction of δ leaves the topology of Fig. 3 unchanged, but there is no stability window now, as $\Omega_1 > \Omega_2$.

A. Topology changes at double roots

As mentioned above, the topology changes in the loci of the three modes occur at a double root. At this point an 'X'-point forms in $\epsilon - \delta$ space and a 'reconnection' occurs between the loci tracks. We can estimate when this happens, as follows.

Starting from eqn.(2), note that at a double root p_d, the dispersion relation must adopt a form where the double root appears quadratically as $(p - p_d)^2$. Consequently, the differential quotient of eqn.(2) with respect to p must also be zero. Performing this operation, and using eqn.(2) again in the resultant expression we find that at a double root

$$4(p - i\Omega)(\epsilon\delta - 1) \;=\; 5(1 - \delta p)(p - \epsilon). \tag{4}$$

Clearly, the dispersion relation itself can also be written as

$$\lambda^5(p-i\Omega)^5(p-\epsilon)^4 \;=\; (1-\delta p)^4. \tag{5}$$

Here p and Ω have been normalised to τ_W, and $\lambda = \tau_L/\tau_W$. Now, introducing $p = \epsilon\hat{p}$, eqns.(4) and (5) together give

$$(1-\epsilon\delta\hat{p})(\hat{p}-1)^9\epsilon^9 \;=\; -\Gamma \;\;,\;\; \Gamma = (4/(5\lambda))^5. \tag{6}$$

As we are only interested in the regime $0 < \epsilon\delta < 0.04$, a good approximation (to be checked *a posteriori*) should be to drop the first factor on the left hand side of eqn.(6) to give an immediate solution for p:

$$p \;=\; \epsilon + \Gamma^{1/9}\exp i\theta_n \;, \tag{7}$$

(where $\theta_n = \pi(1+2n)/9, n = 1,2\ldots$). In a similar vein, the $\epsilon\delta$ term can be dropped from the left hand side of eqn.(4) to find

$$p^2 \;=\; \frac{1}{5\delta}(9p - 4i\Omega - 5\epsilon) \;. \tag{8}$$

A technicality arises concerning the choice of n. This can be traced to the analysis that leads to the particular layer response on the left hand side of eqn.(2). In fact, we must use the imaginary parts of eqns.(7) and (8) to find Ω at a double root, and then find the value of n which ensures that $\mathcal{R}((p-i\Omega)/\Delta')$ and $\mathcal{R}((p-i\Omega)/\Delta')^2)$ are both positive[13] (Δ' is the familiar discontinuity in the logarithmic derivative of the perturbed flux[9]). These conditions ensure that perturbed layer variables asymptote correctly, and so represent physically acceptable solutions. Applying these conditions leads uniquely to $n = 2$, and so we conclude that topology changes in the $\epsilon - \delta$ plane occur at

$$\epsilon \;=\; -\frac{0.92}{\lambda^{10/9}}\delta + \frac{0.35}{\lambda^{5/9}} \;. \tag{9}$$

B. The disappearance of the stability window

We can also find a good approximation for the line in $\epsilon - \delta$ space where the stability window disappears. To do this, recall that at marginality, with $p = i\omega, \omega$ real, eqn.(2) gives

$$\delta\omega^2 + (1-\epsilon\delta)(\sqrt{2}-1)\omega + \epsilon \;=\; 0 \;, \tag{10}$$

and

$$\Omega = \omega - \frac{1}{\lambda}\left[\frac{1+\omega^2\delta^2}{\epsilon^2+\omega^2}\right]^{2/5} . \tag{11}$$

(the physically admissible 1/5 root of -1 implied in eqn.(2) is determined by the same arguments applied in the above subsection). Now, solving the quadratic eqn.(10) for two values of ω and inserting into eqn.(11) we generate two values of Ω, Ω_+ and Ω_-. At the closing of the stability window $\Omega_+ = \Omega_-$, and (employing the approximation $\epsilon\delta << 1$)) we find that the stability window closes along the curve

$$\delta = 0.89\lambda\epsilon^{4/5} . \tag{12}$$

C. Topology of the $\epsilon - \delta$ plane

We are now in a position to collate all this information and summarise the situation with a graph of the $\epsilon - \delta$ plane, with the relevant regions marked out. This is given in Fig. 4.

(In the descriptions that follow, disregard for the time being the two dashed lines of Fig. 4 labelled $\lambda = 1/3$ and 3 as we will discuss the case $\lambda = 1$). Regions D and C possess a stability window in Ω, and undergo a topology change as illustrated across the dotted line (given, with $\lambda = 1$, by eqn.(9)). Regions B and A do not possess a stability window, but similarly have a topology change as illustrated across the same dotted line. Regions B and C are delimited by the disappearance of the stable window (the dashed line labelled $\lambda = 1$ and given by eqn.(12)). We also show the effect of varying the parameter $\lambda = \tau_L/\tau_W$ by giving the lines of vanishing stability window for the cases $\lambda = 1/3$ and 3 as shown. Note that as $\lambda \to 0$ the region possessing a stability window fills the entire $0 < \epsilon\delta < 0.04$ space. This is not surprising, as in this limit, the wall is becoming an increasingly better conductor (we estimate $\lambda \sim 0.2$ in JET).

IV. Torque balance and stability windows

In the preceding section, the plasma bulk velocity was not determined, and remained a free parameter. In this section we first introduce a simple model of torque balance

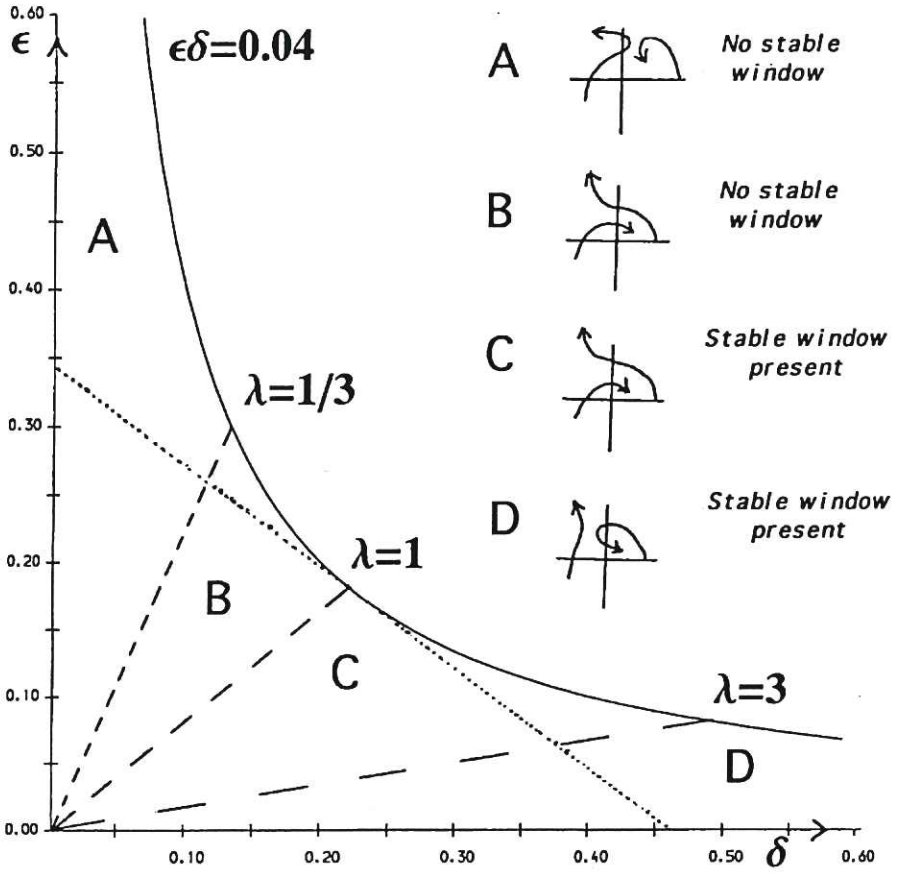

Figure 4: $\epsilon - \delta$ space and topology changes

that determines the plasma flow. This is necessarily a non-linear process as the net electromagnetic torque is quadratic in the perturbation amplitude, and is a function of the mode frequency ω. It is well known that the electromagnetic torque on an ideal MHD fluid is zero, and that torques are only generated across non-ideal MHD layers.[14] Further, the general form for the net electromagnetic torque $\mathcal{T}_{em}$ on a resistive layer obeys

$$\mathcal{T}_{em} \sim (\delta b_r)^2 \mathcal{I}(\Delta') , \tag{13}$$

where δb_r is the perturbed radial magnetic induction, and $\mathcal{I}$ denotes imaginary part. Equation (13) is not unique to plasmas, but is rather a general formula that applies to solid conductors as well.[15] Because of conservation of total torque on the system, we can choose to evaluate eqn.(13) either at the tearing layer, or at the wall. As the wall Δ' has

a particularly simple form ($\Delta'_W = p\tau_W$ so $\mathcal{T}_{em} \propto \omega\tau_W$), we choose to evaluate it there.

This torque has to be balanced against a viscous plasma torque and a given driving torque, the latter being that which gives rotation in the absence of any perturbed fields. So, if Ω_0 is the plasma rotation frequency of an unperturbed plasma equilibrium and Ω is the actual bulk plasma rotation (in the presence of an RWM), the viscous torque will be proportional to the difference between them $\mathcal{T}_{visc} \propto (\Omega_0 - \Omega)$. Accordingly, a simple steady state model of torque balance is

$$\Omega_0 - \Omega \;=\; C\omega \; . \tag{14}$$

Here, ω is the *mode* rotation frequency, in the laboratory frame, normalised to τ_W. The quantity C encapsulates the balance between electromagnetic and viscous torques and will be discussed further below. A variant of this model was used as a basis for successfully interpreting the experimentally observed 'forbidden' bands of plasma rotation on the COMPASS-D tokamak.[16] We can now couple eqn.(14) to the magnetic island/resistive wall system studied in Sec. III. This simply implies that eqn.(14) has to be solved in conjunction with

$$[\lambda(p - i\Omega)]^{5/4} \;=\; \frac{1 - \delta p}{-\epsilon + p} \; . \tag{15}$$

At this level, then, it is apparent that we can expect the system dynamics to be determined by the existence of stability windows and the presence of forbidden bands of plasma rotation.

We will only be interested in those parts of the $\epsilon - \delta$ plane where a stability window exists, so, as a first illustration, we take a case in region D of Fig. 4 and take $\epsilon = 0.05, \delta = 0.5$. Recall that in this region, the RWM by itself displays a stability window, the b and f modes remaining stable. We show the window by tracking the RWM growth rate γ and frequency ω against bulk plasma rotation Ω in Fig. 5.

Note that the stability window (negative γ) occurs in $\Omega_1 = 2.1 < \Omega < 4.5 = \Omega_2$. Now what must be done is to use this record of $\omega(\Omega)$ (lower trace of Fig. 5) in eqn.(14) to produce a graph of Ω against C, for a sequence of different Ω_0. The resulting graph is given in Fig. 6.

We see immediately that despite the apparent simplicity of eqn.(14) (which arises from the choice of referring the torque to the wall), there is multi-valued structure in

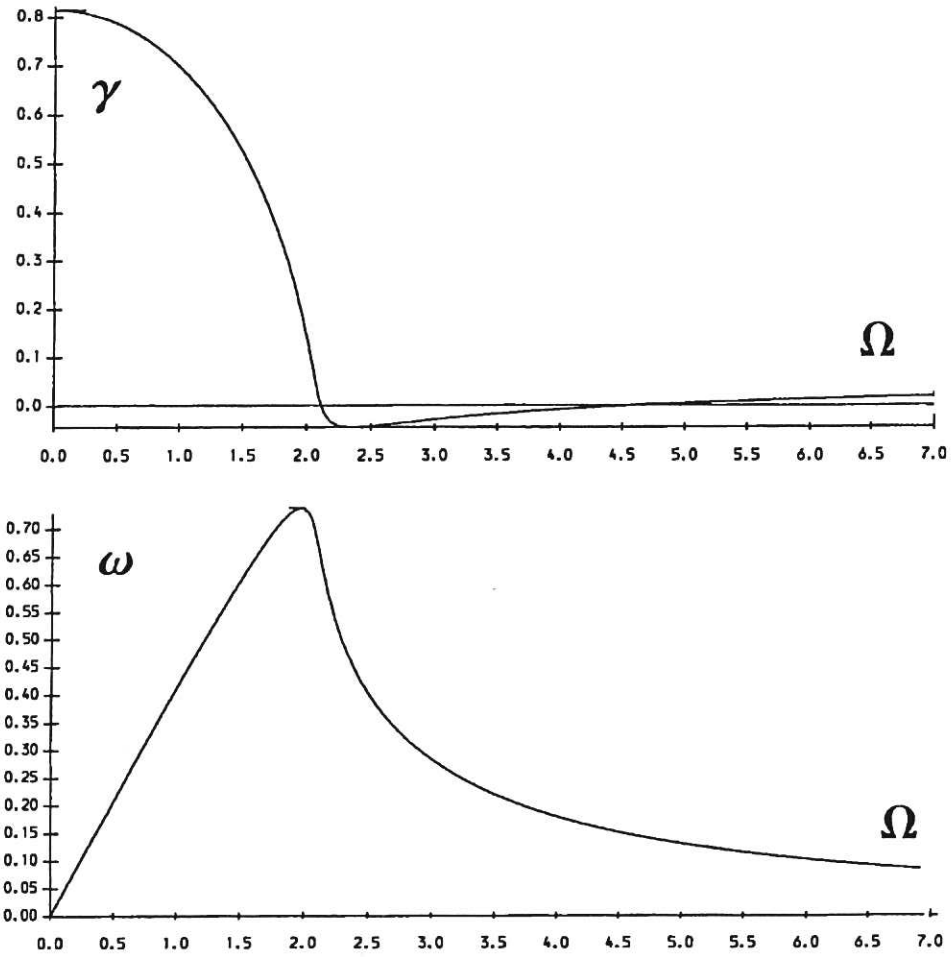

Figure 5: Growth rate and frequency of the RWM against rotation

the result. This multi-valuedness is the direct reason, of course, for the forbidden bands of rotation mentioned above. Various possibilities present themselves. (For guidance in interpreting this graph we have entered the upper and lower limits of the stability window as the two horizontal lines in Fig. 6.) If, for instance, the system is started off with a rotation frequency less than Ω_1, then the RWM is unstable and as the mode grows C will increase while Ω monotonically decreases, asymptoting to zero. (The island size corresponding to the value of C can be estimated using the analysis of Subsection. A below.) This scenario could, in fact, be used to describe the DIII-D experimental result shown in Fig. 1 where mode growth and a decrease of rotation leads to termination of the discharge.

If, of course, the system is started off with $\Omega_1 < \Omega < \Omega_2$ then the system is stable

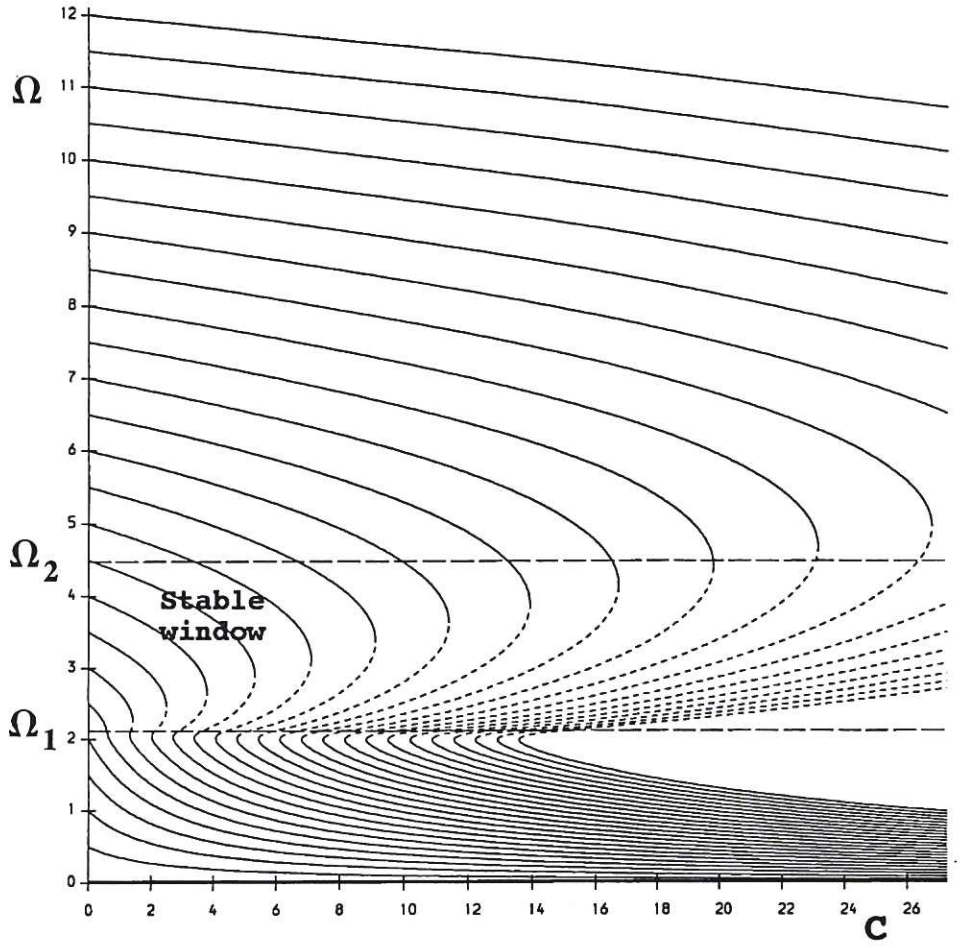

Figure 6: Path of the RWM in $\Omega - C$ space

and would remain in the window. In the case of initiating the system with Ω somewhat greater than Ω_2 then the RWM is again unstable, leading to growth in C. Once more, this will lead to a reduction in Ω, but now this growth will be arrested when Ω drops to the top of the stability window at Ω_2. In this case we see that, at the expense of a saturated island being present in the plasma, the effective stability window has been enlarged (the top boundary of the window has moved from 4.5 to $\sim$ 8, as explained below).

The last possibility in this regime is that which occurs when the initial Ω defines a curve in Fig. 6 for which the top 'knee' is above Ω_2 (this happens whenever the initial Ω is greater than $\sim$ 8 (not shown)). Again, the RWM is unstable, C will increase and Ω decrease until the knee is encountered. At this point, it is well known that the system

does not follow the re-entrant track of the curve (the dotted sections of Fig. 6) as this is unstable.[15,16] Instead, it is forced to migrate vertically down the graph to meet up with the lower branch of the curve. Further, this point (for the ϵ and δ chosen) is beneath the stability window - so that C continues to increase and the island asymptotically locks to the wall.

The second case we consider is one in region C of Fig. 4, by keeping $\epsilon = 0.05$, and changing δ to 0.2. Now, we know from Sec.III that the topology of the window has changed. The window is formed by the RWM stabilising at $\Omega_1 = 2.54$, and the backward b mode destabilising at $\Omega_2 = 4.96$. It follows for this case that *both* modes have to be kept track of. We can produce curves of Ω against C for both modes, and these are shown in Fig. 7.

The top part of Fig. 7 gives the b mode behaviour and the bottom gives the RWM. In both cases we have delineated the stable and unstable parts. It can now be seen that behaviour in the ranges $0 < \Omega < \Omega_1$ and $\Omega_1 < \Omega < \Omega_2$ is entirely analogous to that described in the first example. Then, a similar extension of the stability window occurs above Ω_2. The chief difference between the two topologies arises when that initial value of Ω is encountered which has a track with a top knee above Ω_2. When the system now tracks vertically downwards to a new equilibrium value, the original mode is *stable* and will decay. However, at this point the RWM has become unstable and will start to grow, once more leading to asymptotic locking.

We point out in passing that *if* the bottom branch of an equilibrium lies *inside* the stable window, the modes will decay and C will drop until the equilibrium encounters the bottom knee. Here, the system migrates vertically up in Fig. 6, where again an unstable mode is encountered. In this way there is the intriguing possibility of a 'hysteresis loop' being followed for all time. Other possibilities also present themselves, dependent on the relative positions of the top and bottom knees, Ω_1, Ω_2, and whether the system is in region C or D of Fig. 4.

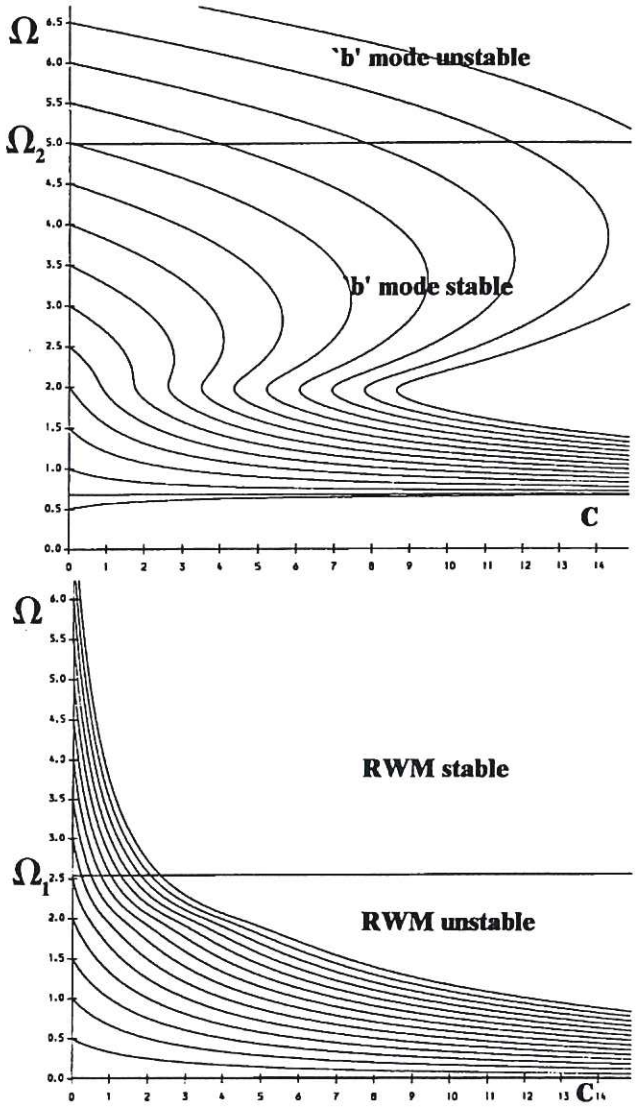

Figure 7: Paths of (top) the 'backward' mode and (bottom) the RWM in $\Omega - C$ space

A. Validity of the tearing approximation

Although the torque balance used in this paper means that the problem is non-linear, we have coupled this with the assumption that the resistive layer is in the linear tearing regime (eqn.(15)). As the island grows, however, and the island size becomes comparable with the tearing layer size, the linear response is then not appropriate and non-linear tearing must be adopted.[17] We can translate this into a condition on the parameter C that appears in eqn.(14). The parameter C is essentially a non-dimensional number that characterises the mode amplitude and the ratio of the viscous to the electromagnetic torques. The viscous torque $\sim \rho_0 \nu v/l$, where ρ_0, ν, and v are, respectively, the plasma

density, kinematic (shear) viscosity, and bulk velocity. l is a characteristic plasma length ($\sim$ the minor radius a). A characteristic viscous damping time is $\tau_V = a^2/\nu$. The electromagnetic torque $\sim (\delta b_W)^2 \Omega \tau_W / \mu_0$ (recall that δb_W is the magnetic perturbation at the wall). We can now find that C is given by

$$C \sim \frac{(\delta b_W)^2 \Omega \tau_W \tau_V}{\mu_0 \rho_0 a v} , \tag{16}$$

and this can be manipulated into the form

$$C \sim \left(\frac{\delta b_W}{B_0}\right)^2 \frac{\tau_W \tau_V}{\tau_A^2} \frac{a}{R_0} , \tag{17}$$

where B_0 is the equilibrium magnetic field strength, τ_A is the characteristic Alfvén time in that field $= a\sqrt{\mu_0 \rho_0}/B_0$, and R_0 is the device major radius.

Now, the island width $W_I \sim a\sqrt{\delta b_L / B_0}$[17] where δb_L is the magnetic perturbation at the resistive layer. The tearing layer width $l_\eta \sim a S^{-2/5}$.[9] Here, S is the Lundquist number given by the ratio of resistive decay time ($\sim a^2/\eta$ with η the plasma resistivity) to τ_A. On assuming a relationship $\delta b_L = f \delta b_W$, the ratio of island to resistive layer width, A, is given by

$$A = \frac{W_I}{l_\eta} = \frac{f^{1/2} \tau_A^{1/2}}{(\tau_W \tau_V)^{1/4}} S^{2/5} \left(\frac{R_0}{a}\right)^{1/4} C^{1/4} , \tag{18}$$

and we note that eqn.(17) can be written

$$C = \left(\frac{W_I}{a}\right)^4 \frac{\tau_W \tau_V}{f^2 \tau_A^2} \left(\frac{a}{R_0}\right) . \tag{19}$$

Now, recall that the limit of linear tearing response occurs at $A \sim 1$. To see what this implies for C we may estimate $S \sim 10^7$ in the outer plasma region, $\tau_A \sim 10^{-7} s$, $\tau_W \sim 10 ms$, and $\tau_V \sim 1 s$. This gives $C \sim (6.3/f^2)(a/R_0)$, and at larger C than this the linear tearing response is not correct. Now, in the nomenclature of Ref. 19, if the mode in question is a 'plasma' mode (approximately moving with the plasma) we have flux suppression at the wall and f will be large. On the other hand, if the mode is a 'wall' mode (approximately locked to the wall) then there is flux suppression at the resistive layer and f will be small. This latter case is thus more likely to be handled correctly by our analysis; it is in fact the primary unstable mode in the system.

V. Conclusions and Discussion

We have investigated a non-linear model of the rotational stabilisation of the Resistive Wall Mode (RWM). Central to the model is a cylindrical plasma that is ideal MHD unstable in the absence of a wall, and tearing stable were the wall perfectly conducting. The question arises as to whether this model is applicable to the full toroidal case. In Finn's original paper Ref. 10(i) he argues that his cylindrical model, which incorporates an internal mode rational surface in the plasma, will be representative of toroidal kink instabilities which must also involve internal mode rational surfaces, because of coupling to poloidal harmonics (ballooning effects). Further, in Ref. 12 it was shown that the exact toroidal dispersion relation for the ideal 'infernal' RWM for a simplified equilibrium is indeed of precisely the same functional form as Finn's (see Ref. 12, eqn.(8)). However, in this case the internal nature of the mode precludes RWM stabilisation. (The infernal tearing mode RWM can be stabilised as its β limit is wall dependent.) In addition, it was shown in Ref. 12 that the dispersion relation for the current driven toroidal kink mode in a more conventional (monotonic q) equilibrium, though not identical to Finn's dispersion relation, is similar (see Ref. 12 eqn.(13)) and displays similar windows of stability in the plasma rotation.

This system then is a qualitative model for the actual toroidal external kink mode that is relevant in Advanced Tokamak scenarios. The rotation frequencies required for RWM stabilisation are of order the inverse wall time (Fig. 5). In the case of DIII-D this translates to a rotation frequency of a few kHz, and this is indeed the observed typical rotation (see Fig. 1). Other theory on RWM stabilisation requires much higher values, typically a few percent of the Alfvén frequency.

However, the model shows that the parameter regime in which stabilisation can take place is small, and would translate into stringent requirements on equilibrium profiles. Essentially, the plasma has to be only slightly ideal unstable in the absence of a wall, and slightly tearing stable were the wall perfect. A non-linear formulation of the problem (with plasma rotation determined self-consistently by an equation of torque balance) indicates that the parameter regime for stabilisation remains small (even more pessimistic statements can be made when the layer response takes into account the effects of averaged

toroidal curvature[18]).

Nevertheless, within this parameter regime, stability windows can be considerably extended at the expense of the growth of a magnetic island. On the other hand, depending on the initial rotation rate, the system can alternatively reduce the plasma rotation asymptotically to zero while the island grows. This appears to be the case in experiments performed on DIII-D. Here, although wall stabilisation of low-n modes based on plasma rotation works (discharges can be sustained for many wall times), once the β limit for the ideal external kink is exceeded, plasma rotation decays and the RWM develops, leading to discharge termination. What is more, in an Advanced Tokamak power plant design, high energy neutral beams will be required for plasma penetration. In this case, the injected momentum density is relatively low.[20] There is a formula available[21] that takes this effect into account and gives a rotation frequency for given device parameters and injection power. We estimate from this that a 'typical' power plant with $\sim 25MW$ of injection power would have a plasma rotation frequency $\sim \mathcal{O}(1)kHz$. To be in the range where Finn stabilisation would occur then requires a wall time constant of only $\sim 5ms$. We stress, however, that as we have seen above, the equilibria that are susceptible to this stabilisation are very tightly constrained. Recall that equilibria were required to be 'slightly' ideal unstable were there no wall, and this is unlikely to be the case at the β_N values (~ 6) found in power plant designs. From all these points of view, it would appear that rotational stabilisation of the RWM in future Advanced Tokamaks can not be relied upon, and some other strategy must be employed.

Feedback stabilisation of *axisymmetric* modes in Tokamaks is now a standard capability.[22] Feedback stabilisation of a *non-axisymmetric* RWM in the HBTX1C RFP was reported in Ref. 23. Here, a specific mode $(m, n) = (1, 2)$ was targeted. Growth of the mode was detected with poloidal field coils, and then dedicated external helical coils were activated. Mode amplitude was successfully suppressed for many wall times (however the overall global plasma confinement properties were not improved).

A scheme for replacing the resistive wall by an active system of current loops (the so-called 'intelligent shell') was proposed in Ref. 24. This was a scheme whereby the current circuits were activated to suppress the flux passing through them and thereby simulating a perfectly conducting wall. This scheme would of course seek to suppress all

RWMs, not just ones with a specific helicity. The idea was further developed in Ref. 20, where a number of autonomous feedback loops covering a fraction of the wall area was used.

A further possibility for stabilising all RWMs was suggested in Ref. 25. Here a rotating secondary wall was envisaged (simulating a flowing lithium blanket). The RWM clearly cannot lock to both walls simultaneously, and a condition on the wall rotation frequency for RWM stabilisation was found to be

$$\Omega \sim \mathcal{O}(1/\tau_{W1}) + \mathcal{O}(1/\tau_{W2}) , \tag{20}$$

so the required rotation rate is determined largely by the inverse time constant of the least conducting wall. (Essentially, this is the same effect that led to eqn. (1).) It was found that the requirement on the *position* of the secondary rotating wall was that it should be within the marginal point of the most unstable mode that exists with no wall. Recently, this idea has been further developed in Ref. 26 where it was shown that a network of conductors external to the plasma could be so configured as to simulate the rotating secondary wall of Ref. 25 - the so-called 'fake' rotating wall. As found in Ref. 25, the rotation rate is determined by the fake wall's inverse time constant, and the fake wall has to be located within the marginal point of the most unstable mode without a wall. In practice, this is a difficulty as power plant designs demand that any feedback devices be placed outside the blanket. However, Ref. 27 demonstrated that the fake wall could be 'projected' within the critical radius even though the actual hardware was well outside it. Reference 27 also stated that the gain, bandwidth, current and total power requirements of the feedback system could be estimated as less than a hundred, a few Hz, a few tens of kA and a few MW respectively. These requirements are within the scope of present technology. This scheme, then, which is more efficient than the intelligent shell proposal, would appear to be more power plant relevant than the approach of inducing bulk plasma rotation.

Acknowledgment.

This work was funded jointly by the UK DTI and EURATOM.

References

[1]C. Kessel, J. Manickam, G. Rewoldt, and W. M. Tang, Phys. Rev. Lett. **72**, 1212 (1994).

[2]J. Manickam, M. S. Chance, S. C. Jardin, C. Kessel, D. Monticello, N. Pomphrey, A. Reimann, C. Wang, and L. E. Zakharov, Phys. Plasmas **1**, 1601 (1994).

[3]A. Bondeson, M. Benda , M. Persson, and M. S. Chu, Nucl. Fusion **37**, 1419 (1997).

[4]C. G. Gimblett, Nucl. Fusion **26**, 617 (1986).

[5]B. Alper, M. K. Bevir, H. A. B. Bodin, C. A. Bunting, P. G. Carolan, J. Cunnane, D. E. Evans, C. G. Gimblett, R. J. Hayden, T. C. Hender, A. Lazaros, R. W. Moses, A. A. Newton, P. G. Noonan, R. Paccagnella, A. Patel, H. Y. W. Tsui, and P. D. Wilcock, Plasma Phys. Control. Fusion **31**, 205 (1989).

[6]P. Greene and S. Robertson, Phys. Fluids ΘB **5**, 556 (1993).

[7]R. R. Goforth, T. N. Carlstrom, C. Chu, B. Curwen, D. Graumman, P. S. C. Lee, E. J. Nilles, T. Ohkawa, M. J. Schaffer, T. Tamano, P. L. Taylor, T. S. Taylor, and D. F. Register, Nucl. Fusion **26**, 515 (1986).

[8]J. A. Wesson, Phys. Plasmas **5**, 3816 (1998).

[9]H. P. Furth, J. Killeen, and M. N. Rosenbluth, Phys. Fluids **6**, 459 (1963).

[10](i) J. M. Finn, Phys. Plasmas **2**, 198 (1995).
(ii) J. M. Finn, Phys. Plasmas **2**, 3782 (1995).

[11]T. S. Taylor, Phys. Plasmas **2**, 2390 (1995).

[12]C. G. Gimblett and R. J. Hastie, in *Theory of Fusion Plasmas* (edited by J W Connor, E Sindoni and J Vaclavik), Editrice Compositori, Bologna 1999, 319.

[13]C. G. Gimblett, in *Physics of Mirrors, Reversed Field Pinches and Compact Tori* (edited by S Ortolani and E Sindoni), Editrice Compositori, Bologna 1988, **1**, 241.

[14]R. Fitzpatrick, R. J. Hastie, T. J. Martin, and C. M. Roach, Nucl. Fusion **33**, 1533 (1993).

[15]C. G. Gimblett and R. S. Peckover, Proc. Roy. Soc. A **368**, 75 (1979).

[16]D. A. Gates and T. C. Hender, Nucl. Fusion **36**, 273 (1996).

[17]P. H. Rutherford, Phys. Fluids **16**, 1903 (1973).

[18]A. Bondeson, C. G. Gimblett, and R. J. Hastie, Phys. Plasmas **6**, 637 (1999).

[19]A. Bondeson A and H. X. Xie, Phys. Plasmas **4**, 2081 (1997).

[20]T. H. Jensen and R. Fitzpatrick, Phys. Plasmas **4**, 2997 (1997).

[21]ITER Physics Basis, Chap. 2, to appear in Nucl. Fusion.

[22]E. A. Lazarus, J. B. Lister, and G. H. Nelson, Nucl. Fusion **30**, 111 (1990).

[23]B. Alper, Phys. Fluids B **2**, 1338 (1990).

[24]C. M. Bishop, Plasma Phys. Contr. Fusion **31**, 1179 (1989).

[25]C. G. Gimblett, Plasma Phys. Contr. Fusion **31**, 2183 (1989).

[26]T. H. Jensen and R. Fitzpatrick, Phys. Plasmas **3**, 2641 (1996).

[27]R. Fitzpatrick, Phys. Plasmas **4**, 2519 (1997).